



Chaotic Motion in the Outer Asteroid Belt and its
Relation to the Age of the Solar System

Marc A. Murison, Myron Lecar, and Fred A. Franklin

Harvard-Smithsonian Center for Astrophysics

60 Garden Street

Cambridge, MA 02138

email: murison,lecar, or franklin@cfa.harvard.edu

As published in the *Astronomical Journal* 1994, **108**, 2323.

ABSTRACT

Recently, we analyzed a relation, found for chaotic orbits, between the Lyapunov time T_L (the inverse of the maximum Lyapunov exponent) and the "event" time T_e (the time at which an orbit becomes clearly unstable). In this paper we treat two new problems. First, we apply this T_L - T_e relation to numerical integrations of 25 outer-belt asteroids and show that, when viewed in the proper context of a Gaussian distribution of event time residuals, none of the 25 objects exhibits an anomalously short Lyapunov time. The current age of the solar system is approximately three standard deviations or less from the anticipated event times of all of these asteroids. We argue that the Lyapunov times of the 25 remaining bodies are each consistent with the age of the solar system, and that we are therefore seeing the remnants of a larger original distribution. The bulk of that population has been ejected by Jupiter, leaving the "tail members" as present-day survivors. This interpretation is consistent with current understanding of the behavior of trajectories near KAM tori in Hamiltonian systems. In particular, there is no need to invoke a new type of motion or class of dynamical objects to explain the short Lyapunov timescales found for solar system objects.

Second, we discuss integrations of 440 fictitious outer-belt asteroids and show that the slope and offset parameters of the T_L - T_e relation do not change with an increase in Jupiter's mass by a factor of 10, and that the distribution of residuals in $\log T_e$ is Gaussian. This allows us to sensibly and *quantitatively* interpret the significance of the Lyapunov timescale. However, the width of the residuals distribution is a function of mass ratio. Since knowledge of the distribution width is needed in order to interpret the significance of predicted event times, a calibration must be performed at the mass ratio of interest.

I. INTRODUCTION

Strikingly large values of the maximum Lyapunov exponent are associated with chaotic motion in the solar system (e.g. Sussman and Wisdom 1988, 1992; Laskar 1989; Torbett 1989; Mikkola and Innanen 1992). In this paper, we continue our efforts to interpret the Lyapunov time, $T_L=1/\gamma$, in the solar system in light of a relation between T_L and the "event" time T_e (Soper et al. 1990; Lecar et al. 1992a; Lecar et al. 1992b, henceforth LFM; Levison and Duncan 1992; Holman and Wisdom 1993):

$$\log \frac{T_e}{T_0} = a + b \log \frac{T_L}{T_0} \quad (1)$$

where T_0 is an appropriate normalizing period. The event time is the timescale on which the qualitative character of the motion changes. Events are indicated by, for example, a close approach to a planet, the crossing of a planetary orbit, or the escape of a satellite – in general, an ejection or a collision. We use the notation T_e , rather than T_c , the planetary orbit crossing time (Lecar et al., 1992a), to reflect this more generalized meaning of an event. For this study, $T_0=T_J$, the orbital period of Jupiter. Notice that, unlike the slope b , the value of the offset parameter a scales with T_0 . For orbits interior to Jupiter, we find in this paper that $a=1.30 \pm 0.03$ and $b=1.74 \pm 0.03$, in good agreement with the preliminary results of LFM. The T_L - T_e relation is the only known method for *prediction* of the long-term instability timescale of solar-system bodies.

Here we focus our attention primarily on two issues. First, we have calculated T_L for all 25 known outer-belt asteroids not associated with a major resonance ($3.43 < a < 3.76$ AU).

Just beyond the upper limit of the range considered here are the Hilda group asteroids. See Franklin et al. (1993) for further discussion and an application of the T_L - T_e relation to these interesting objects. The Lyapunov times of the 25 orbits considered here range from 3200 yr to greater than 96,000 yr. We interpret these values in terms of the T_L - T_e relation and argue that the few remaining bodies with short T_L are the expected remnants of an initially much larger population. An alternative view (Milani and Nobili, 1992), that existing bodies with short T_L are members of a curious class of objects described by the misleading label "stable chaos," seems unlikely. The existence of this purported class was inferred on the basis of numerical integrations of a single body, (522) Helga, and is, we claim, a misinterpretation of the significance of the observed T_L . Our interpretation is in fact consistent with well-established behavior of trajectories near invariant surfaces of Hamiltonian systems.

The T_L - T_e relation suffers from being poorly established for times greater than 10^{6-7} Jovian periods. Levison and Duncan (1992) have completed some integrations for up to 4 Gyr in the region of the proposed Kuiper belt, and their results appear to follow the T_L - T_e relation. (They also report, for integrations between Jupiter and Saturn and between Uranus and Neptune, approximate values of $a \approx 1.4$, $b \approx 1.9$, in good agreement with our values.) However, encouraging as these results are, there is still an insufficient number of $T_e > 10^6 T_0$ orbits calculated to date. Since the needed long-term integrations are difficult to obtain, we also investigate here the conse-

quences of increasing Jupiter's mass to speed up perturbation effects.

II. METHOD

The dynamical system utilized for this study is the three-dimensional elliptic restricted three-body (ERTB) problem, with Jupiter as the secondary mass m_2 . We integrated the equations of motion in the rotating-pulsating frame (cf. Szebehely 1967, Szebehely and Giacaglia 1964) with a Bulirsch-Stoer extrapolation method (e.g. Stoer and Bulirsch 1980, Press et al. 1992). See Murison (1989) for details on the numerical performance of the integrator. The (constant) eccentricity used for Jupiter in all cases was $e_J=0.04848$. This model is convenient because of its simplicity. The ERTB problem is the simplest dynamical model which is still complex enough to exhibit all the important behavior required for this study. Comparisons with a model that includes the effects of Saturn on the motion of Jupiter (cf. Lecar and Franklin, 1973) yielded no significant differences that would affect our results in the region of the asteroid belt considered here. In particular, an integration of (2311) El Leoncito yielded a T_L of 460 T_J , fully consistent with our value of 422 T_J . Relying on a reasonable and simple statistical interpretation, as well as indications from recent nonlinear dynamics literature, we conjecture that the property of certain orbits to exhibit long-term "stability" despite short Lyapunov times is in fact to be expected, as we argue in the next section.

Along with each orbit, a second "test" orbit was integrated. This second orbit started a distance 10^{-6} in phase space from the reference orbit and was used for calculating the

Lyapunov exponent. Renormalization of the test orbit with respect to the reference orbit occurred whenever the phase space distance exceeded 10^{-4} , thus avoiding saturation problems. See e.g. Benettin et al. (1976) and Wolf et al. (1985) for details on calculating Lyapunov exponents.

We obtained orbital elements for the 25 known outer-belt asteroids not associated with a low-order resonance from the Minor Planet Center for the epoch JD 2448601.0 = 10 Dec. 1991. The orientation elements were transformed to Jupiter's orbital plane, in order to determine the correct ERTB initial conditions. The original and transformed elements are shown in Table I. Elements for Jupiter were taken from Danby (1988).

We performed numerical integrations for each of the 25 asteroids. Predicted event times were determined by application of the T_L - T_e relation, eq. (1), to the calculated Lyapunov exponent. The length of these integrations was 10^5 Jovian years (~ 1.2 Myr) – sufficient to determine whether or not the predicted event time is within several standard deviations of the age of the solar system, T_{SS} . Longer integrations, though certainly possible, are in fact unnecessary, since the shortest Lyapunov times (those most likely to be in serious disagreement with the age of the solar system) are accurately calculated.

In order to investigate the T_L - T_e relation for a high mass ratio, we integrated 440 fictitious outer-belt orbits over a wide range of initial semimajor axis with $m_2=10 M_J$. The initial eccentricity of these orbits was 0.05, the longitude of pericenter 320 deg, inclination 3 deg,

Chaotic Motion in the Outer Asteroid Belt

Table I. Initial orbital elements of the 25 outer-belt asteroids with respect to the equator and equinox of 2000.0 and at epoch JD 2448601.0 = 10 Dec. 1991. Primed elements are with respect to the Jovian orbital plane.

	Asteroid	M	i	Ω	ω	e	a/a _J	i'	Ω'	ω'
1144	Oda	297	9.65	157.64	222.17	0.08	0.72	9.01	150.36	215.15
2311	El Leoncito	218.11	6.63	157.45	181.53	0.05	0.70	6.02	153.67	171.04
522	Helga	355.81	4.45	117.52	249.06	0.08	0.70	3.23	110.14	242.22
2932	Kempchinsky	234.52	2.24	169.84	187.71	0.11	0.69	2.16	190.03	153.29
2697	Albina	82.78	3.59	273.26	121.67	0.09	0.68	4.89	260.95	119.77
721	Tabora	328.98	8.34	39.39	359.22	0.12	0.68	7.79	16.83	7.66
3092	Herodotus	238.78	10.88	9.37	0.11	0.11	0.68	10.98	348.43	6.97
1990WK		113.58	10.37	73.93	254.27	0.10	0.68	9.22	56.16	257.9
1574	Meyer	186.5	14.4	246.93	259.35	0.05	0.68	15.5	235.33	256.66
909	Ulla	85.56	18.84	147.28	230.13	0.10	0.68	17.97	136.01	227.04
3095	Omarkhayyam	215.01	2.98	293.81	119.46	0.06	0.67	4.26	275.54	123.54
414	Liriope	257.68	9.58	111.46	329.74	0.08	0.67	8.30	98.97	328.01
536	Merapi	19.55	19.44	59.78	304.97	0.09	0.67	18.47	43.04	307.65
2208	Pushkin	351.61	5.42	79.71	346.15	0.05	0.67	4.23	59.27	352.41
87	Sylvia	10.11	10.87	73.75	272.95	0.08	0.67	9.72	56.14	276.41
1328	Devota	42.47	5.78	224.04	169.27	0.15	0.67	6.59	219.28	159.77
107	Camilla	260.39	9.92	174.15	296.52	0.08	0.67	9.64	167.34	289.02
260	Huberta	169.49	6.42	165.97	173.45	0.12	0.66	6.00	163.14	162.02
121	Hermione	126.25	7.54	74.59	289.17	0.14	0.66	6.39	55.32	294.27
4236		23.95	7.32	349.32	162.48	0.03	0.66	7.88	326.29	171.39
2634	James Bradley	211.55	6.44	134.48	340.07	0.07	0.66	5.41	128.01	332.29
2196	Ellicott	28.19	10.28	212.59	319.15	0.06	0.66	10.84	204.71	312.72
1390	Abastumani	277.93	19.98	29.54	1.91	0.03	0.66	19.59	11.88	5.59
2702		181.74	1.59	247.02	311.08	0.08	0.66	2.77	247.8	296.09
65	Cybele	144.44	3.54	156.05	109.27	0.1	0.66	3	162.82	88.26
Jupiter:		M = 135.417073,	i = 1.303713,	Ω = 100.382152,	ω = 273.819181,	e = 0.04848169,				
		a = 5.21021558,	v = 137.300833							

true anomaly 40 deg, and the semimajor axis ranged from 0.659 to 0.750 a_J . Aside from the semimajor axes, these particular values were arbitrarily chosen. The eccentricity of the primaries was $e_2 = e_J$. The maximum length of the integrations was 10^6 Jovian years (~ 12 Myr), and an event was presumed to have occurred if

$r_{Sun} > 1.1 a_J$ (5.73 AU) for more than one Jovian year. The larger mass ratio allowed perturbations to develop faster and therefore quicker acquisition of results.

III. RESULTS

Outer-Belt Asteroids and Long-Term Chaotic Motion

We present our results for the 25 outer-belt asteroid integrations in Table II. Times are in units of Jupiter periods T_J (11.86 yr). The Lyapunov time T_L is shown in column 3, while the predicted escape time T_e , in units of $10^6 T_J$, is in column 4. T_e was calculated from eq. (1) using $b=1.74$ and $a=1.30$. These values were determined from the semimajor axis survey results of this study, presented below. They agree with the values found in LFM for asteroid orbits interior to Jupiter. The 25 orbits fall into three categories, as denoted in column 5. An "A" signifies a clearly chaotic orbit, where

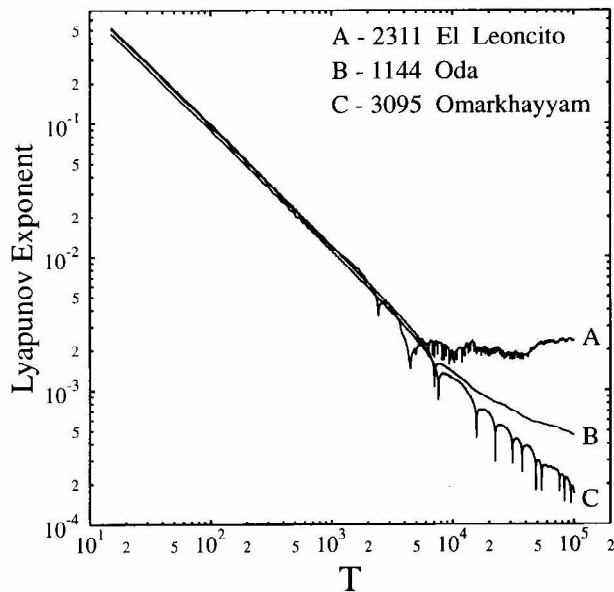


Figure 1. Typical behavior of the Lyapunov exponent γ as a function of time (in Jovian periods), illustrating three types. The curve labeled A is strongly chaotic; an approximate value for γ is quickly found. Curve B is "possibly-chaotic," and further integration is required to determine the asymptotic value of γ . Curve C represents a typical quasiperiodic (or at best very weakly chaotic) orbit.

the Lyapunov exponent as a function of time appears to have leveled off to a nonzero value. A typical plot of γ in such a case is shown in Figure 1, curve A. A "B" in column 5 signifies a probable chaotic orbit, where γ appears to be leveling off but the integration was not long enough to determine a value. The values of T_L calculated for these orbits are therefore lower limits. A typical plot for this case is shown in Figure 1, curve B. A "C" in column 5 means that the orbit was quasiperiodic (or very weakly chaotic at best), where the Lyapunov exponent is asymptotically zero (or nearly zero). Curve C of Figure 1 shows γ vs. t for a typical orbit of this type. The actual T_L for these orbits is very large. We could have performed longer integrations and, possibly, thereby removed some of the $>$ signs from columns containing T_L and T_e – i.e., converted class C into class B, or class B into class A. This would be a noble deed, but not an especially valuable use of time because our real interest and concern centers on just those minor planets with short Lyapunov times.

An important characterization of the T_L - T_e relation is the width of the distribution of orbits about the best fit to eq. (1). It may be used to interpret the significance of a given value of T_L and therefore relate it to physical systems. In data obtained from LFM, we found that the distribution of residuals in $\log T_e$ for the Jupiter-Sun system and asteroid orbits inside Jupiter's orbit was consistent with a Gaussian shape with standard deviation $\sigma = 0.98$. Thus, for a given population of objects, some nonzero percentage would be expected to lie in the tail of the distribution. Take for example the asteroid in Table II with the

Chaotic Motion in the Outer Asteroid Belt

Table II. Results of 25 outer-belt asteroid integrations. Times are in Jovian orbital periods. See text for the meaning of σ . Final column lists the most significant resonance encompassed by the observed range in semimajor axis (see text).

Asteroid	T_L	$T_e (10^6)$	σ	resonance		
1144	Oda	>2100	>12.75	B	<1.50	13:8
2311	El Leoncito	422	0.75	A	2.76	12:7
522	Helga	>2915	>21.74	B	<1.27	12:7
2932	Kempchinsky	>1900	>9.86	B	<1.62	12:7
2697	Albina	>2500	>16.07	B	<1.40	16:9
721	Tabora	2,299	14.37	A	1.45	16:9
3092	Herodotus	2,421	15.73	A	1.41	16:9
1990W		2,564	17.38	A	1.37	16:9
1574	Meyer	3,717	33.22	A	1.08	16:9
909	Ulla	>2600	>17.31	B	<1.37	16:9
3095	Omarkhayyam	>4900	>54.29	C	<0.86	20:11
414	Liriope	>3000	>23.02	C	<1.24	20:11
536	Merapi	2,801	20.28	A	1.3	20:11
2208	Pushkin	>4400	>45.03	B	<0.94	20:11
87	Sylvia	>8100	>128.27	C	<0.48	20:11
1328	Devota	287	0.38	A	3.06	20:11
107	Camilla	3,145	24.82	A	1.21	11:6
260	Huberta	270	0.34	A	3.1	13:7
121	Hermione	3,571	30.98	A	1.11	13:7
4236		2,841	20.79	A	1.29	13:7
2634	James Bradley	>3700	>33.02	B	<1.08	13:7
2196	Ellicott	>3200	>25.95	B	<1.19	15:8
1390	Abastumani	>5000	>54.75	C	<0.86	****
2702		2,463	16.21	A	1.4	15:8
65	Cybele	299	0.41	A	3.03	15:8

shortest Lyapunov time, (260) Huberta, with $T_L=270 T_J$ and $T_e=323,000 T_J$. The age of the solar system, $T_{SS} = 3.78 \times 10^8 T_J = 4.5$ Gyr, corresponds to a residual of $\log T_{SS} - \log T_e = 3.07 = 3.13 \sigma$. We claim that this apparently small value of T_L , and the corresponding T_e , is *not* in significant conflict with objects still being present after a time of order T_{SS} . One could argue

that (260) Huberta belongs to the tail of a population distributed around the mean defined by eq. (1). Knowledge of this prevents a serious misinterpretation of T_L .

Our values for σ are lower limits; the longer the asteroids remain in their present orbits, the more significant will be their deviation from the mean relation eq. (1). If our interpretation is

correct, we would expect that an original population of asteroids would be largely depleted by now, leaving a few members in the large- T_e tail as present-day survivors. We have thus quantitatively determined the short- T_L boundary for this type of object. If this boundary were inconsistent with the age of the solar system, we would be faced with a quandary. However, we argue that this is not the case.

Recently, Milani and Nobili (1992) reported an integration of just one outer-belt asteroid, (522) Helga. They found a Lyapunov time of roughly $T_L=580 T_J$ (6900 yr). Unaware of the

actual significance of this value, they claimed discovery of (522) Helga as the first known example of a new class of dynamical behavior for which they contrived the misleading and ill-considered label "stable chaos." They go on to claim that T_L in this case must therefore be "meaningless." However, using our initial conditions we find $T_L > 2915 T_J$, corresponding to only 1.3σ from T_{SS} for T_e . With slight changes in the initial conditions (cf. Figure 2), we were able to drop (522) Helga into the 12:7 resonance with Jupiter, finding an average value in the resonance of $T_L=490 T_J$, which is even smaller than, but comparable to, Milani and Nobili's value and corresponds to $T_e \approx 950,000 T_J$. (The similarity of our value for T_L , obtained with the ERTB equations of motion, and Milani and Nobili's value, resulting from integration of all the planets, lends further support for our use of the simpler ERTB problem.) Yet even this value of T_e is only 2.7σ from T_{SS} . Thus we find it difficult to believe that the longevity of (522) Helga despite an apparently short T_L is evidence of a new class of objects or a new physical concept. Rather, it is more likely that Helga is a tail member of the distribution of residuals in T_e about the mean T_L - T_e relation eq. (1). Indeed, we conjecture that (522) Helga is *not* stable, and that it will eventually suffer a catastrophic change in its orbit (cf. Wisdom, 1983, figs. 1 and 4). We argue this point in more detail below.

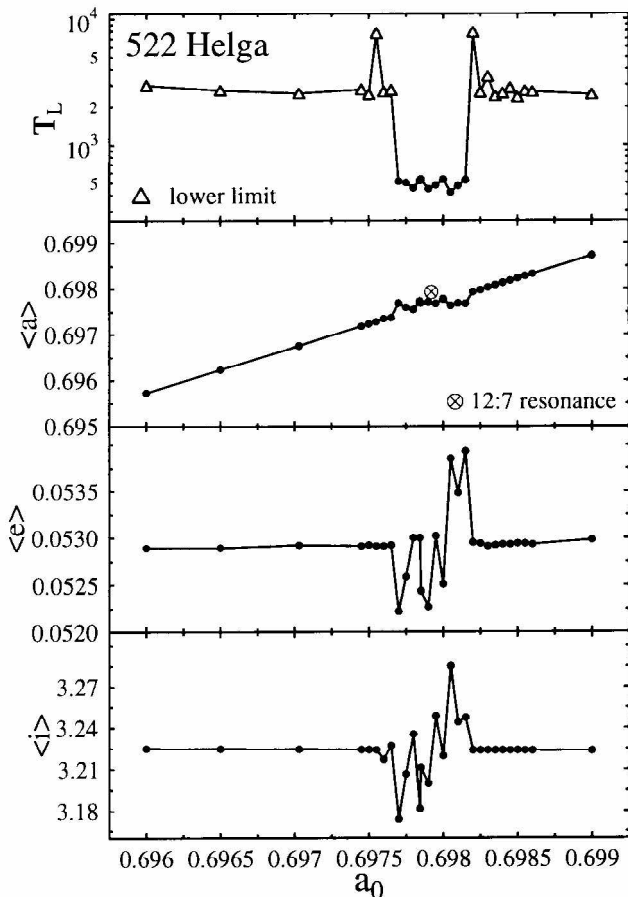


Figure 2. Variation of T_L with initial semimajor axis for (522) Helga (top panel). Successive panels show the variation of the semimajor axis, orbital eccentricity, and orbital inclination, averaged over the integration time of $10 T_J$.

The next to last column of Table II shows the number of standard deviations that the age of the solar system lies from the expected value for T_e as calculated from T_L and the T_L - T_e relation. Of the clearly-chaotic orbits, for which we can calculate a reliable T_e , three asteroids

are close to three standard deviations (asteroids 1328, 260, and 65), one is at 2.8σ , and the rest lie well within 2σ . This distribution is consistent with the notion that in the outer-belt asteroids we are seeing the remnants of a larger original distribution. The bulk of that population has been cleared out by Jupiter, leaving the long- T_e tail members to survive to the present.

The observed value of γ fluctuates with small changes of the initial conditions. For example, Figure 2 shows the Lyapunov timescale as a function of initial semimajor axis for (522) Helga. The value of T_L is greater than 32,000 yr (corresponding to $T_e \sim 22$ Myr), except in a narrow interval around the 12:7 resonance, $a_0 \in [0.69770, 0.69815]$, where T_L averages about 5800 yr ($T_e \sim 0.95$ Myr). The open triangles denote a lower limit, since the Lyapunov exponent in these cases did not level off to a definite value by the end of the integration (cf. curves A and B of Figure 1). Also shown in Figure 2 are the corresponding mean values of semimajor axis, eccentricity, and inclination, averaged over the length of the integrations ($100,000 T_J$). The 12:7 mean motion resonance is at $a=0.697922 a_J$, marked by the symbol in the second panel of Figure 2. We noted variations in T_L of roughly 12 percent within the resonance. The chaos exhibited by the motion of (522) Helga is apparently associated with the 12:7 resonance, and the semimajor axis width of this resonance is clearly delineated by the behavior of T_L , the mean eccentricity, and the mean inclination. The last column in Table II shows the nearest mean motion resonance encompassed by the given orbit over the length of the $10^5 T_J$ integrations. Those with short Lyapunov times are, like

(522) Helga, possibly associated with the corresponding resonance for the particular initial conditions we used. The range in semimajor axis for (522) Helga was more than a factor of 7 larger than the width of the resonance as evidenced in Figure 2. Asteroid (1390) Abastumani, falling between 15:8 and 13:7, was the only one whose semimajor axis did not at any time in our numerical integration cross a resonance. (This asteroid exhibited behavior consistent with quasiperiodic motion, cf. Table II.) We are not certain to what extent, if any, the asteroids are affected by the corresponding resonances, but the association is suggestive (see below).

An Interpretation of Short Lyapunov Times

We propose the following picture for the dynamics leading to an "event." First we review briefly the relevant dynamics of a two degree of freedom system, then we conjecture that analogous behavior is occurring in the much more complicated, many degree of freedom, Hamiltonian system represented by the outer-belt asteroids.

It is well-known that, in a two degree of freedom Hamiltonian system, invariant surfaces (KAM tori) divide the phase space. Under the influence of a sufficiently strong perturbation, the "outermost" invariant surfaces are destroyed, giving rise to a global sea of chaos surrounding an inner stable region, where invariant surfaces still exist. At the core of the stable region is a stable period one orbit. Further out, past the outermost intact surface and embedded in the chaotic sea, are secondary invariant surfaces surrounding elliptic period n

orbits. Each of these period n islands has associated with it a similar hierarchy of higher-order island chains, and so on.

Consider an outermost intact invariant surface. A sufficient increase in the magnitude of the perturbations will produce a tear in this surface. Under dynamical evolution of the surface, this tear will propagate and reproduce over the surface, producing a fractal distribution (Cantor set) of holes or gaps, known as a cantorus (Percival, 1979; MacKay et al., 1984). The surface is not completely destroyed, but neither is it any longer impervious to diffusion of orbits across it. There is a countable infinity of holes. The stronger the perturbation(s), the more "porous" is the cantorus. Thus, it is possible for an orbit to be trapped in a region of phase space, enclosed by a cantorus of small porosity, for some time before encountering a "hole" and escaping into a more unstable region. Some orbits may escape quickly; others will be trapped for some time. Given an initial population of such orbits, one would expect a distribution of escape times – perhaps Gaussian. The same argument can be used for orbits near the secondary islands, which themselves will be enclosed by cantori (and higher-order islands, etc.).

Analytic calculation of diffusion rates across hierarchies of cantori is very difficult. As a trajectory passes through a cantorus, it may be derailed to "shadow" a higher-order island chain, which itself has a grid of cantori gaps, and so on. Numerically, it can be shown that the distribution of orbits initially in the neighborhood of an island remaining in that neighborhood (i.e., the "survival" probability) is

$$P(t) \sim t^{-\beta} \quad (2)$$

for long times t (normalized by the orbit period), where $\beta \approx 1.4$ for a small, isolated island (Chirikov and Shepelyansky, 1984b; Karney, 1983; Lichtenberg and Lieberman, 1992). For the main island of the standard map (Chirikov, 1979), $\beta \approx 1.45$ (Chirikov and Shepelyansky, 1984a; Murray, 1991). It would be reasonable to wonder if the tori surrounding regular islands is the main barrier to diffusion of a trajectory outward. However, it appears that the sticking time to a given surface is the dominant process in impeding phase space transport (Chirikov and Shepelyansky, 1984a,b; Murray, 1991). The departures of diffusion from unimpeded random motion are due to a small percentage of orbits that are stuck around KAM surfaces bounding a region of chaotic motion.

We may associate an escape past a particular cantorus with an "event" in an asteroid orbit, since (going back to the two degree of freedom analogy) successive cantori are rapidly more porous, leading quickly to the global sea of chaos and therefore wild excursions of the orbit. We propose that this is a reasonable possibility for the mechanism displayed by the outer-belt asteroids. The foregoing has been well-established for simpler Hamiltonian systems (cf. Lichtenberg and Lieberman, 1992; Wiggins, 1990).

An alternative view is that KAM tori are "sticky." Karney (1983) was the first to numerically study the stickiness of KAM tori, finding that long-time correlation functions for a version of the standard mapping are strongly governed by the dynamics near KAM surfaces.

It has often been observed that orbits near an invariant surface become "trapped" into almost regular orbits for long (but finite) times (Perry and Wiggins, 1994; Kaneko and Konishi, 1994; also Wisdom, 1983). Jensen (1984, a review) and Lai et al. (1992, recent work) apply this to the surviving fraction of un-ionized atoms in a model of the ionization of surface-state electrons in an oscillating electromagnetic field. Such "stickiness" will have a profound effect on the statistical properties of a system, including diffusion rates or escape rates. A population of trajectories will contain some members lying closer than others to a KAM surface, leading to a distribution of escape times, some of which will be long.

Perry and Wiggins (1994) show that the survival probability for an N-degree of freedom

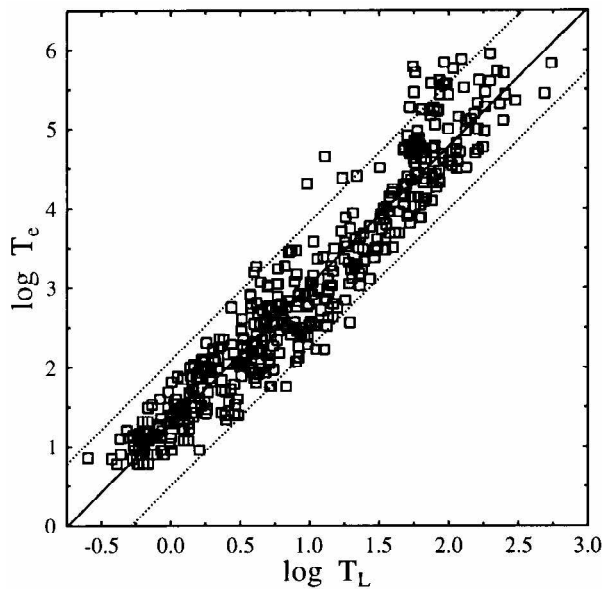


Figure 3. Log of observed event time, T_e , vs. the log of the Lyapunov time, T_L , for the 440 survey orbits calculated with $m_2=10 M_J$. The solid line is an unweighted least squares fit, with slope $b=1.74 \pm 0.03$ and intercept $a=1.30 \pm 0.03$. Dotted lines mark the $2\sigma_G$ boundaries of a Gaussian fit to the residuals.

Hamiltonian depends strongly on the dynamics near the KAM tori. Solutions beginning there simply take a long time to move away, despite the fact that the motion is chaotic. They rigorously derive a lower bound on the time it takes to move away from a torus:

$$T \geq \frac{C}{r} e^{(K\beta/r)^\alpha} \quad (3)$$

where T is the lower bound on the time it takes to double the distance from the surface, r is the distance from the surface, C and K are positive constants that depend on the analytic properties of the Hamiltonian, $\beta > 0$ is a measure of the irrationality of the flow, $\alpha = 1/(N+2)$, and N is the number of degrees of freedom. The more irrational the flow (i.e., the higher the resonance order), the more "sticky" is the surface. Lower bounds like this were first obtained by Nekhoroshev (1977) for a class of near-integrable Hamiltonian systems and are therefore known as Nekhoroshev type bounds. They were worked out for the time to move away from elliptic equilibrium points by Giorgilli (1988) and Giorgilli et al. (1989).

The extension to the outer-belt asteroids follows naturally, and we do not therefore require the existence of some mysterious, new class of objects or type of motion in order to explain the observed behavior. It is, in fact, quite consistent with the above-mentioned previous studies. The association with KAM tori also explains our observation that the outer asteroid orbits considered here all lie near a high-order resonance with Jupiter, the main perturber.

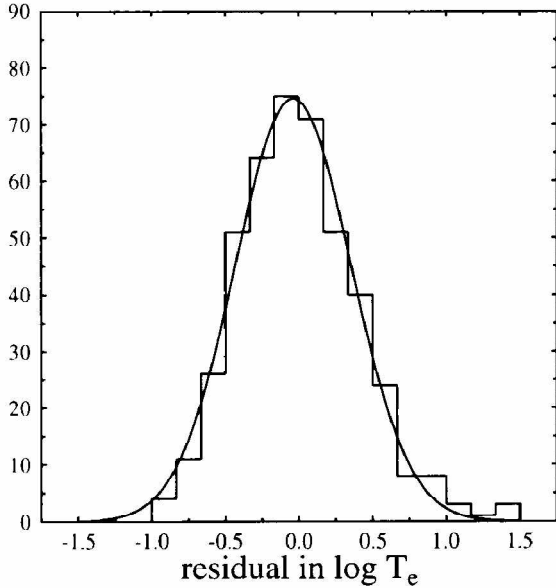


Figure 4. Histogram of the difference of $\log T_e$ (observed event time) from the linear fit to the semimajor axis survey data (solid line) of Figure 3. Smooth curve is the best-fit Gaussian, with $\sigma_G=0.39$.

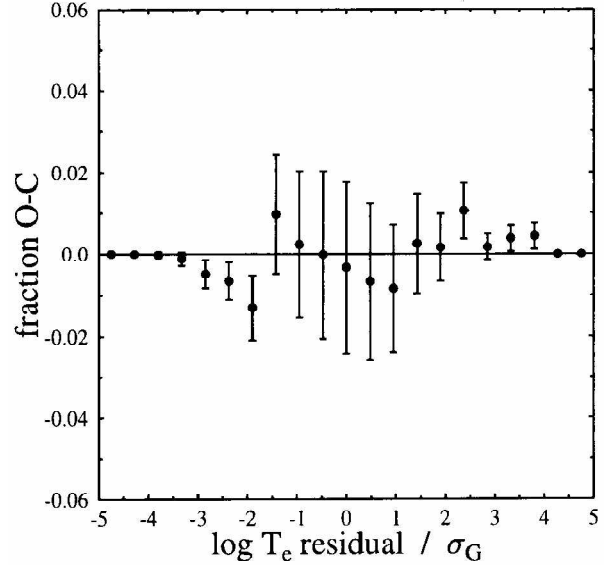


Figure 5. Difference between observed and expected fraction of data points falling into histogram bins of Figure 4, for a Gaussian distribution. Error bars are $\pm 1\sigma$.

Semimajor Axis Survey and Residuals Distribution

The results of a semimajor axis survey with $m_2 = 10 M_J$ are displayed in Figure 3. The solid line is the unweighted least squares fit to 440 orbits, with slope $b=1.74 \pm 0.03$ and intercept $a=1.30 \pm 0.03$ (all quoted errors are 1σ formal uncertainties). The standard deviation of the residuals is $\sigma = 0.41$. Agreement with the LFM values for orbits interior to Jupiter ($b=1.73 \pm 0.19$, $a=1.53 \pm 0.34$) is well within the formal uncertainties. This agreement illustrates the apparent robustness of the relation. It appears that a and b are insensitive to the mass ratio for this dynamical configuration.

The distribution of the data points in $\log T_e$ from the least squares fit (i.e., the residuals) is approximately Gaussian. Figure 4 is a histogram of the distance in $\log T_e$ from the solid

line in Figure 3. The smooth curve in Figure 4 is the best-fit Gaussian to the histogram data. It was found that the best fit is achieved by excluding the "bump" in the right-hand tail (represented by four orbits near 1.4). With standard deviation and mean as free parameters, we find $\mu=-0.039$ and $\sigma_G=0.39$, which is reassuringly close to the RMS deviation, $\sigma = 0.41$. A more quantitative view of the fit of the histogram data to a Gaussian is shown in Figure 5. Here we show the difference between the observed and expected fraction of data points falling into the histogram bins. The error bars are $\pm 1\sigma$ and represent the error in the fraction, which is proportional to \sqrt{n} (and not the fractional error, which goes as $1/\sqrt{n}$). The abscissa is the residual in units of σ_G . There are no significant deviations, including the points in the tail that were excluded in the

fit. We also calculated the skewness S of the distribution (all data included), finding $S/\sigma_S = 2.6$, where $\sigma_S = \sqrt{15/N}$ is the theoretical standard deviation for the skewness of an ideal Gaussian distribution. It is difficult to interpret the significance of a nonzero skewness, since it is highly sensitive to the tail, which in turn suffers from small number statistics. A value 2.6 standard deviations from the expected is possibly significant.

The nonzero skewness of our distribution arises almost entirely from the presence of the four orbits making up the bump near 1.4 in Figure 4. Removing these orbits drops the skewness to approximately one standard deviation from a perfect Gaussian. Are these four orbits anomalous, or do they just represent statistical fluctuations? One can ask this question: given the expected number of orbits in a particular bin, what is the probability of finding the observed number? One may also adjust bin width to gauge sensitivity to bin boundary placement. For the bump orbits, that probability ranges, depending on bin boundaries, from six to eighteen percent – not unreasonably small, and relatively insensitive to bin width. Nevertheless, we reintegrated these orbits with microscopically different initial conditions and found that they shifted out of the tail, removing the bump. As a further check, we then reintegrated seven other orbits chosen at random from the distribution and observed the same kind of movement within the distribution. Thus, we conclude that the noise in T_L is such that, in this distribution of only 440 points, features like the small bump in Figure 4 are statistical fluctuations.

The dotted lines in Figure 3 mark the $2\sigma_G$ boundaries of the Gaussian fit. The standard deviation of this distribution is almost a factor of three smaller than the σ calculated from the LFM data involving Jupiter at its actual mass. Thus, the distribution width is a function of mass ratio. It is also apparent from the figures in LFM that σ is an increasing function of orbital inclination of the test particle.

Summary

We have examined the 25 "non-resonant" outer-belt asteroids in light of the T_L - T_e relation and found that their predicted event times, though significantly less than the age of the solar system T_{SS} , are statistically consistent with their being present today. The key to this conclusion is that chaotic orbits are, to a close approximation, normally distributed about the mean T_L - T_e relation for the particular mass ratio and dynamical configuration in question. We think that the 25 objects are the expected distribution tail of an originally much larger population, which has been thinned out by Jupiter. The adjustable parameters of the T_L - T_e relation are relatively insensitive to mass ratio and dynamical configuration. However, the distribution width – crucial for interpreting the significance of predicted event times – is a function of the mass ratio. We have noted the existence of one such misinterpretation in the recent literature, and we urge caution to the dynamical community to prevent such mistakes in the future.

The two facets of the problem discussed in this paper compliment each other in the following sense. Despite the fact that the distribution width is a function of the mass ratio, Figures 3

Chaotic Motion in the Outer Asteroid Belt

and 4 for the 10 M_J case clearly show that some bodies further than $\sim 2\sigma$ from the relation are present. We suggest, therefore, that the minor planets in the outer belt with short T_L (and $T_e < T_{SS}$) are the counterparts of these bodies for the real, $1M_J$ case.

We thank Brian Marsden and Gareth Williams of the Minor Planet Center for their usual cheerful and prompt responses to requests for asteroidephemerides.

REFERENCES

- Benettin, G., Galgani, L., and Streleyn, J.-M. (1976). *Phys. Rev. A* **14**, 2338.
- Brouwer, D., and Van Woerkom, A.J.J. (1950). *Astron. Papers Amer. Eph. Naut. Almanac* **13**, 81.
- Chirikov, B.V. (1979). *Phys. Rep.* **52**, 263.
- Chirikov, B.V., and Shepelyansky, D.L. (1984a). Proc. 9th Int. Conf. on Nonlinear Oscillations (Kiev), Vol. II (Naukova Dumka, Kiev). English translation: Plasma Physics Lab. Rep. PPPL-TRANS-133, Princeton Univ.
- Chirikov, B.V., and Shepelyansky, D.L. (1984b). *Physica D* **13**, 395.
- Danby, J.M.A. (1988). *Fundamentals of Celestial Mechanics*, 2nd edition, Willmann-Bell, Richmond.
- Franklin, F., Lecar, M., and Murison, M. (1993). *Astron. J.*, **105**, 2336.
- Giorgilli, A. (1988). *Ann. Inst. Henri Poincare* **48** A, 423.
- Giorgilli, A., Delshams, E., Foutich, E., Galgani, L., and Simo, C. (1989). *J. Diff. Eq.* **77**, 167.
- Holman, M.J., and Wisdom, J. (1993). *Astron. J.* **105**, 1987.
- Jensen, R.V. (1984). *Phys. Rev. A* **30**, 386.
- Kaneko, K., and Konishi, T. (1994). *Physica D* **71**, 146.
- Karney, C.F.F., (1983). *Physica D* **8**, 360.
- Lai, Y.C., Grebogi, C., Blumel, R., and Ding, M. (1992). *Phys. Rev. A* **45**, 8284.
- Laskar, J. (1989). *Nature* **338**, 237.
- Lecar, M., and Franklin, F. (1973). *Icarus* **20**, 422.
- Lecar, M., Franklin, F., and Soper, P. (1992a). *Icarus* **96**, 234.
- Lecar, M., Franklin, F., and Murison, M. [LFM] (1992b). *Astron. J.* **104**, 1230.
- Levison, H.F., and Duncan, M.J. (1992). Preprint.
- Lichtenberg, A.J., and Leiberman, M.A. (1992). *Regular and Chaotic Dynamics*, 2nd ed., Springer-Verlag, New York.
- MacKay, R.S., Meiss, J.D., and Percival, I.C. (1984). *Physica D* **13**, 55.
- Mikkola, S., and Innanen, K. (1992). *Astron. J.* **104**, 1641.
- Milani, A., and Nobili, A. (1992). *Nature* **357**, 569.
- Murison, M., (1989). *Astron. J.* **97**, 1496.
- Murray, N.W. (1991). *Physica D* **52**, 220.
- Nekhoroshev, N.N. (1977). *Russ. Math. Surv.* **32**, 5.
- Percival, I.C. (1979). In *Nonlinear Dynamics and the Beam-Beam Interaction*, eds. M. Month and J.C. Herrera, Am. Inst. of Physics Conf. Proc. No. 57.
- Perry, A.D., and Wiggins, S. (1994). *Physica D* **71**, 102.
- Press, W.H., Flannery, B.P., Teukolsky, S.A., and Vetterling, W.T. (1992). *Numerical Recipes in C: The Art of Scientific Computing*, 2nd edition, Cambridge Univ. Press, New York.
- Soper, P., Franklin, F., and Lecar, M. (1990). *Icarus* **87**, 265.
- Stoer, J., and Bulirsch, R. (1980). *Introduction to Numerical Analysis*, Springer-Verlag, New York.
- Sussman, G.J., and Wisdom, J. (1988). *Science* **241**, 433.
- Sussman, G.J., and Wisdom, J. (1992). *Science* **257**, 56.
- Szebehely, V. (1967). *Theory of Orbits*, Academic, New York.
- Szebehely, V., and Giacaglia, G.O. (1964). *Astron. J.* **69**, 230.
- Torbett, M.V. (1989). *Astron. J.* **98**, 1477.
- Wiggins, S. (1990). *Introduction to Applied Nonlinear Dynamical Systems and Chaos*, Springer-Verlag, New York.
- Wisdom, J. (1983). *Icarus* **56**, 51.
- Wolf, A., Swift, J.B., Swinney, H.L., and Vasano, J.A. (1985). *Physica D* **16**, 285.